GEOHORIZON

Three-dimensional kinematic modeling of reversible fault and fold development

Natacha Gibergues, Muriel Thibaut, and Jean-Pierre Gratier

ABSTRACT

In the current context of continuous supply of energy, the discovery and development of new prospects will rely on our ability to detect reserves in deeper and structurally more complex formations. These exploration areas stretch the capabilities of currently available three-dimensional (3-D) exploration software, which cannot accommodate a realistic geometrical description of present-day geological structures and the tectonic deformation steps. Correctly handling the kinematics of structural deformation and evaluating the pressure regime and temperature history at the scale of exploration will remain as challenges for several years to come. In this article, we focus on geometric aspects using a reversible kinematic approach to deform and restore faulted and folded structures. Kinematic modeling is a good alternative to the complexity of a mechanical approach and is sufficiently representative of the natural processes involved (sedimentation, erosion, and compaction). Its reversibility ensures that the basin parameters need to be defined only once for both the restoration and the deformation steps. The model describes the incremental development of the basin in space and time. It is based on a hexahedral discretization process that is fully adapted and appropriate for thermal and fluid transfer. Different deformation modes (flexural slip and vertical shear) are mixed to integrate natural deformation more effectively. The algorithm is validated using different geological examples of growing complexity up to curved normal and thrust faults. The approach offers various prospects for

Manuscript received October 3, 2008; provisional acceptance February 2, 2009; revised manuscript received April 29, 2009; final acceptance June 1, 2009.

DOI:10.1306/06010908130

AUTHORS

Natacha Gibergues ~ *Institut Français du Pétrole, Av. de Bois Préau, BP 311, Rueil-Malmaison 92506, France; natacha.gibergues@yahoo.fr*

Natacha Gibergues has a Ph.D. from Joseph Fourier University, Grenoble (2007). She has worked for the ALTRAN company from 2007 to 2009.

Muriel Thibaut ~ *Institut Français du Pétrole, Av. de Bois Préau, BP 311, Rueil-Malmaison 92506, France; muriel.thibaut@ifp.fr*

Muriel Thibaut has worked with the Institut Français du Pétrole since 2001. In 2006, she was the project leader responsible for defining the strategy for basin software. Her recent work includes defining the methodology for coupling complex tectonics with fluids. She received her Ph.D. in geometry and solid mechanics from the University of Grenoble in 1994.

Jean-Pierre Gratier ~ *Laboratoire de Géophysique Interne et Tectonophysique, CNRS-Observatoire, Université Joseph Fourier, Géosciences, BP 53X, Grenoble 38041, France; Jean-Pierre.Gratier@obs.ujf-grenoble.fr*

Jean-Pierre Gratier is professor, physicist of observatory, at the Joseph Fourier University, Grenoble. He received his Ph.D. in geology in 1973. He works on the mechanisms of creep and sealing in the upper crust both from experimental approaches and from analysis of natural processes. His recent work is focused on fault permeability and strength evolution related to earthquakes and fluid transfers.

ACKNOWLEDGEMENTS

The authors acknowledge the permission given by the Institut Français du Pétrole to publish this article. This article greatly benefited from reviews made by J. F. Gale and S. E. Laubach. The AAPG Editor thanks the following reviewers for their work on this paper: Julia F. Gale, Stephen E. Laubach, and an anonymous reviewer.

improvement, integrating both kinematic and mechanical constraints. Considering the challenges that the industry needs to overcome in future exploration, the results of this approach are very encouraging and can be considered as a solution for solving the structural part of 3-D basin modeling in complex areas.

INTRODUCTION

In view of the current context of oil and gas exploration, the development of new prospects will depend on our ability to detect reserves in increasingly complex geological environments. Petroleum system evaluation and basin modeling tools are required to improve knowledge of hydrocarbon potential in mature and underexplored areas. Such evaluation calls for knowledge of both the present-day basin and its deformation history because of the need to couple dynamic changes in the basin with the simulation of fluid migration. The basin modeling tool must handle the coupling between the reconstructed geometry through geological time and the controlling physical processes that lead to the generation and migration of hydrocarbons. Difficulties occur, however, in considering a realistic geometric description of geological structures at the present day and during the tectonic deformation steps. Coupling an understanding of petroleum systems with the precise kinematics of structural deformation is still a challenge in three-dimensional (3-D) modeling. Three-dimensional software tools simulating fluid flow coupled with dynamic geometry through time already exist. However, changes in geometry, to represent the restoration of the structures from a deformed to an undeformed state, are described by vertical decompaction, named backstripping (Schneider et al., 2000). In these software tools, faults are virtual and are only represented by their hydraulic properties. In two-dimensional (2-D) modeling, software tools exist that can consider more complex and realistic geometries, including faults (Schneider et al., 2002). However, considering the function of the fault network in 3-D is much more complicated, and some research still needs to be done (Thibaut et al., 2007). In 3-D, when the history of the structural basin cannot be described satisfactorily with vertical decompaction, the hypothesis of backstripping is too restrictive; for example, fault movements may be crucial to explaining the creation of hydrocarbon traps, or the time scale of tectonic episodes may explain the time scale of maturation. In these cases, a more rigorous analysis of structural deformation using restoration methods needs to be done to define the deformation path. Various surface restoration methods have been proposed for simple shear (Gibbs, 1983) or flexural slip (Gratier et al., 1991; Gratier and Guillier, 1993; Samson, 1996; Williams et al., 1997). Some methods are especially devoted to integrating heterogeneous strain such as fault termination and noncylindrical folds (Rouby et al., 1993; Cognot et al., 2001; Dunbar and Cook, 2003; Caumont et al., 2004). With regard to volumetric restoration, some solutions have been proposed using a mechanical approach (Maerten et al., 2001; Galera et al., 2003; Moretti et al., 2006) or a kinematic approach (Divies, 1997; Cornu et al., 2003). For a 3-D basin modeling study in a structurally complex area, keeping the same gridding model for both the restoration step and the simulation step is potentially interesting in terms of the efficiency and accuracy of the entire process governing petroleum formation. However, this implies certain compromises. Mechanical restoration has the advantage of integrating the mechanical properties of the rocks, but the basic tetrahedral shape of the gridding is not well suited to the numerical simulation of fluid migration. In contrast, with a kinematic approach, the use of hexahedral gridding is an advantage for 3-D fluid migration simulation (see the Discussion section). This article presents a reversible kinematic approach using a single gridded model for both the restoration step (named the inverse step) and the development of the geological structures. The solution is an acceptable way of describing deformation from the present-day (deformed) structure to the restored (undeformed) structure and then back to the present structure. In this approach, the path is not only reversible and geometric but also incremental in time, which is different from those approaches that unfold instantly in one step from the present-day structure to the structure at the time of deposition (Gratier and Guillier, 1993; Bennis et al., 1995; Rouby et al., 2000; Thibert et al., 2005). The advantage of a step-by-step process is that it can consider the changes in certain parameters during the progressive deformation (i.e., deposition and erosion, compaction, permeability, etc.). The use of a fracture-mechanics-based crack-growth simulator (Philip et al., 2005) is, for example, an interesting complementary approach to evaluate the evolution of permeability. In 2-D, software tools exist to describe incremental kinematics (Suppe, 1983; Contreras and Sutter, 1990; Divies, 1997), and some initial solutions have been published in 3-D (Cornu et al., 2003; Moretti et al., 2006). In the approach presented here, the goal is to offer a suitable mesh for both restoration and simulation that can be used for the thermal history; the deformation of rock properties such as sedimentation, erosion, and compaction; and fluid transfer. This approach is based on the work of Cornu et al. (2003). We used the geometric method that was validated on examples limited to one deformable unit overthrusting a fixed basement. In this article, the approach has been generalized with more than two deformable units and integrates two mechanisms of deformation: vertical shear and flexural slip (Gibergues, 2007). Additionally, reversibility was implemented and validated using different cases. The results give a coherent kinematic mesh between the deformed and the undeformed state, which is suited to fluid transfer modeling. The results of this work are a first step toward solving 3-D basin modeling in complex settings.

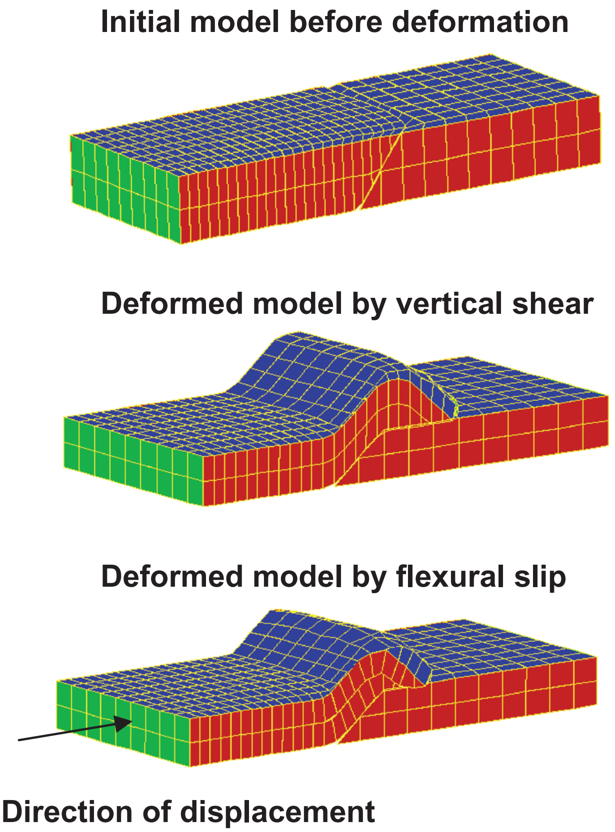

Figure 1. Different mechanisms of deformation that can be used in modeling: vertical shear and flexural slip.

PRINCIPLES OF THE METHOD

The method adopts the following assumptions with regard to the definition of the basin:

- The basin is divided into several units (i.e., blocks) separated by faults and subdivided into layers of constant thickness in the initial state.
- Fault locations are known a priori, and no sealing properties are attached to the faults.
- The layers slide perfectly, which means slip between them is frictionless.
- The layers slip independently of one another. Considering a different type of behavior for each layer of rock by choosing a deformation mechanism is possible: vertical shear or flexural slip. With the vertical shear method, the restoration vectors are parallel to the vertical direction. Layer thickness is not preserved through the restoration. This deformation mode is relevant to so-called incompetent layers (Ramsay and Huber, 1987). With the flexural method, the layer thickness is preserved and the deformation mode is relevant to geological observations of the deformation of so-called competent layers (Figure 1).
- The basin has an imposed lateral border, defined as a plane surface. The boundary condition is fixed during deformation and delimits the lateral slip of the basin.

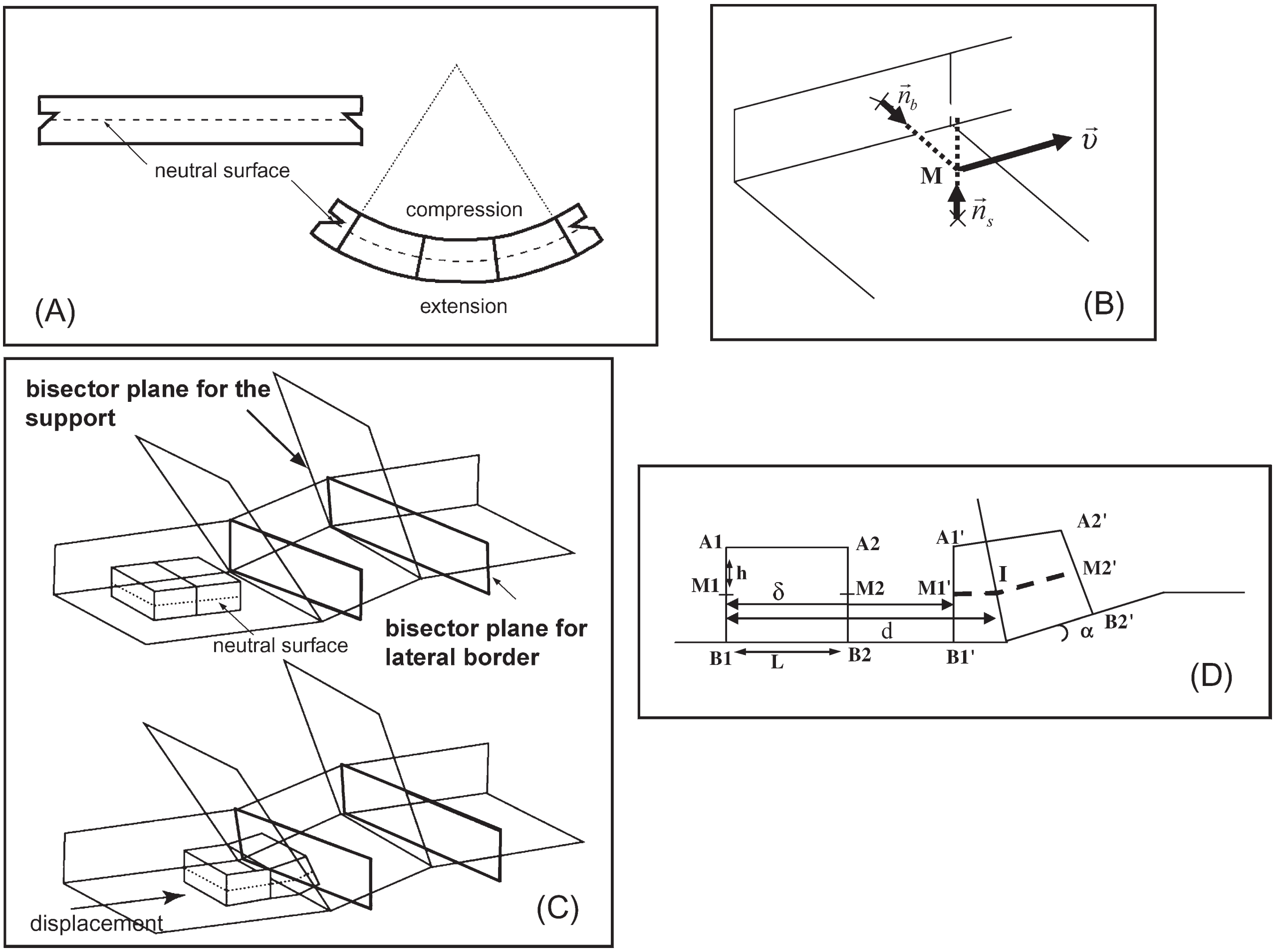

Figure 2. (A) Fixed neutral surface in a deformed layer. (B) Definition of the displacement direction $\vec{\upsilon}$ for a point M of the neutral surface, with $\vec{n}_s$, the vector normal to the support, and $\vec{n}_b$, the vector normal to the imposed lateral boundary. (C) Diagram showing the displacement of a rigid block. (D) Representation in cross section of an element climbing a ramp: α is the angle between the slope of the support and the horizontal plane, L is the length, h the half height of the element, d is the Euclidean distance between I and M_1, I is the introspection point with the bisector plane, and M_1' is the location of M_1 after displacement.

- The sliding support is defined as being the top of the basement for the first layer, and the top of the previous layer for the upper layers. It is extended to the whole domain with the top of the other blocks when a multiblock basin is considered.
- The area of the neutral surface is preserved as well as possible during deformation in the case of vertical shear and exactly in the case of flexural slip. The neutral surface is that which separates the thickness of the layer into two equivalent sublayers: one being extended toward the exterior curve and the other being compressed toward the interior curve. From the geometrical point of view, the neutral surface is considered as being undeformable and remains parallel to the sliding support during the progressive deformation (Figure 2A). From the discrete point of view, the neutral surface remains parallel as far as possible when crossing a breaking point (Figure 2D). A layer is displaced by displacing all the points of the neutral surface.
- A layer is partitioned into rigid quadrilateral blocks (3-D hexahedra), which move by translation and rotation. Internal deformation is local and located at the breaking point where the slope changes. Empty and recovered spaces observed in the model are interpreted as being physical processes that have occurred at small scales, such as

for example pressure solution creep and sealing processes. Pressure solution is seen to accommodate both folding processes and interseismic fault displacement (Groshong, 1975; Laubsher, 1975; Gratier and Gueydan, 2007) and compaction processes (Dewers and Ortoleva, 1990).

The objective of this kinematic approach is to use as much as possible the properties of the neutral surface to describe the progressive deformation of the layers. The problem is less difficult when considering the properties of the neutral surface because instead of deforming volumetric elements, the model deforms superimposed surfaces. Using a multilayer model with different deformation modes for the layers (vertical shear versus flexural slip) is also more realistic than using homogeneous behavior for the entire formation because in natural deformation the partition between various modes of deformation most commonly occurs at the scale of the sedimentary layers. Consequently, multilayered 3-D modeling with mixed deformation modes is necessary in considering the complexity of the geological processes. However, limited computational capability prevents us from modeling this contrasted multilayered behavior when it occurs at small scales (superimposed decimeter layers with contrasted deformation modes). With present computational capability, the deformation mode must be homogenized in layers of the various formations about a hectometer thick. This is still realistic for modeling folding and fracturing of such formations (Ramsay, 1967; Ramsay and Huber, 1987). To model geological series with contrasted deformation modes, the first step is therefore to identify the main mechanism of deformation for hectometer-thick formations. A simple way to do this is, for example, to distinguish on a drilled core between formations that show no evidence of change in thickness and can be modeled by the flexural method, and formations that display internal deformation, for example, with cleavage development, that can be modeled by vertical shear. The hypothesis of rigidity is represented by preserving the height of the edge of each elementary block as the layer is deformed (Figure 2). Each edge is rebuilt by translation and rotation across the neutral surface. Depending on the deformation mode chosen, the height of the edge is preserved vertically, in the case of vertical shear, or perpendicular to the sliding support, in the case of flexural slip, to preserve the thickness of the layer (Figure 1). The unknowns of the problem are the coordinates of the nodes of the neutral surface after displacement. If the displacement is defined by the curvilinear translation vector $\vec{\upsilon}$ (Figure 2B), $\vec{\upsilon} = \vec{n}_s \wedge \vec{n}_b$, where $\vec{n}_s$ is the vector normal to the support and $\vec{n}_b$ is the vector normal to the imposed lateral boundary, a point $M_1(x_1, y_1, z_1)$ of the neutral surface moves parallel to the sliding support along a line D (M_1, $\vec{\upsilon}$) with a displacement of length δ (Figure 2D). Point M_1 moves along line D until the neutral surface crosses the first bisector plane (the bisector plane linked to the lateral imposed boundary or that attached to the sliding support) (Figure 2C). Considering point I of the intersection between line D and the bisector plane and d the Euclidean distance between points I and M_1, point M_1 has to move by an amount d. Three possibilities exist:

1. $\delta < d$, the coordinates of the new point $M_1^{'}$ are $M_1^{'} = \begin{cases} x_1 + \vec{\upsilon}_x\delta \\ y_1 + \vec{\upsilon}_y\delta \\ z_1 + \vec{\upsilon}_z\delta \end{cases}$
2. $\delta = d$, point $M_1^{'}$ is the same as point I
3. $\delta > d$, $M_1^{'}$ moves to I, hence a distance $\delta - d$.

After the displacement of the neutral surface, the second step of deformation is to rebuild the edges by rigid rotation around the neutral surface. One important relationship to consider in building the mesh is that between the length of an element and the slope of the ramp to be climbed. This relationship aims at preventing the edges from crossing during displacement, which means that the thickness and length of the element are linked by the following equation:

$$L \geq h \ \tan\ \alpha, \forall\ \alpha\ \in [0; \pi/2] \qquad (1)$$

The relationship emphasizes the fact that it is impossible to get up a ramp with a slope greater than $\pi/2$ (Figure 2D).

APPLICATIONS

The examples are presented in order of growing geological complexity to emphasize the potential of the approach.

Coupling of Different Modes of Deformation in an Example with a Variable Ramp

As a first example, we present the results of coupling different modes of deformation (vertical shear and flexural slip). This example represents a basin described by two units of four layers each, an imposed vertical lateral boundary, and a curved ramp with a slope varying laterally (Figure 3A, B). Displacement is in the x direction, and the length of displacement is 2000 m (6562 ft) (Figure 3C). The enlargement in Figure 3D checks the orientation of the edges as a function of the deformation mode. The first and third layers are deformed by flexural slip: the edges are perpendicular to the sliding support. The second and fourth layers are deformed by vertical shear: the edges remain parallel to the vertical direction. Lateral sliding of the third layer can be observed because of the curved ramp. Figure 3E represents the relative volumetric variation $\Delta V = (V_{\mathrm{d}} - V_{\mathrm{i}})/V_{\mathrm{i}}$ before (V_{i}) and after (V_{d}) the imposed displacement for each cell of the first and second layers. The results are consistent with the hypotheses of the associated deformation. In the case of the first layer, deformed by flexural slip, the local volumetric variation is less than a few percent, which is compatible with the conservation of the thickness of the layer. In the case of the second layer, deformed by vertical shear, the volumetric variation is of the same order, but the variation increases on climbing the ramp.

Reversibility in an Example of a Basin Described by Several Units Deformed by Flexural Slip

The following example aims at testing the reversibility of the approach using a multiblock basin. The initial model gridding is an important step because it must verify that no edge crosses (equation 1) over the entire kinematic range. This condition imposes a relationship between the length and height of each cell (but also between the width and height). The relationship linking the height with the length or width of a cell has an impact on the number of cells required for the model to represent a specific thickness. The size of a cell also has an impact on the numerical precision of the computation. A compromise must be found between the computation time and the precision to be attained in describing the displacement of the model. The cylindrical model is composed of a fixed basement and two mobile and thrusting units (Figure 4). The chronology of displacement between the different units is the following. In Figure 4A, two units (2 and 3) are displaced and thrust over the basement (unit 1) by two successive displacements of 3000 then 4000 m (9842 then 13,123 ft) in the x direction. In Figure 4B, the two units (2 and 3) are restored after two 5000-m (16,404-ft) displacements to their initial state at the time of deposition. Reversibility is ensured because the solution of the inverse problem (Figure 4A) after a displacement of 10,000 m (32,808 ft) is close to the initial direct simulation model (Figure 4B). The total volume variation for the deformation step before and after displacement is less than 1.9%, which is due to some cells being compressed and others elongated.

Example of a Geological Basin of Realistic Complexity Deformed by Gravity

The last example is inspired by the structures located in the Gulf of Mexico (Rowan et al., 1999) (Figure 5A). The basin is composed of three units separated by a normal and two thrust faults. The imposed lateral boundary is interpreted as being a strike fault. Figure 5B and C illustrate the 3-D model, showing a bird's-eye view and cross section. The chronology of displacement between the different units is the following: two units (2 and 3) are displaced and thrust over the basement (unit 1) by successive displacements in the x direction.

The layers of the model are deformed by flexural slip. Figure 6A represents the initial state before deformation. Figure 6B represents the deformed model after a displacement in the x direction of

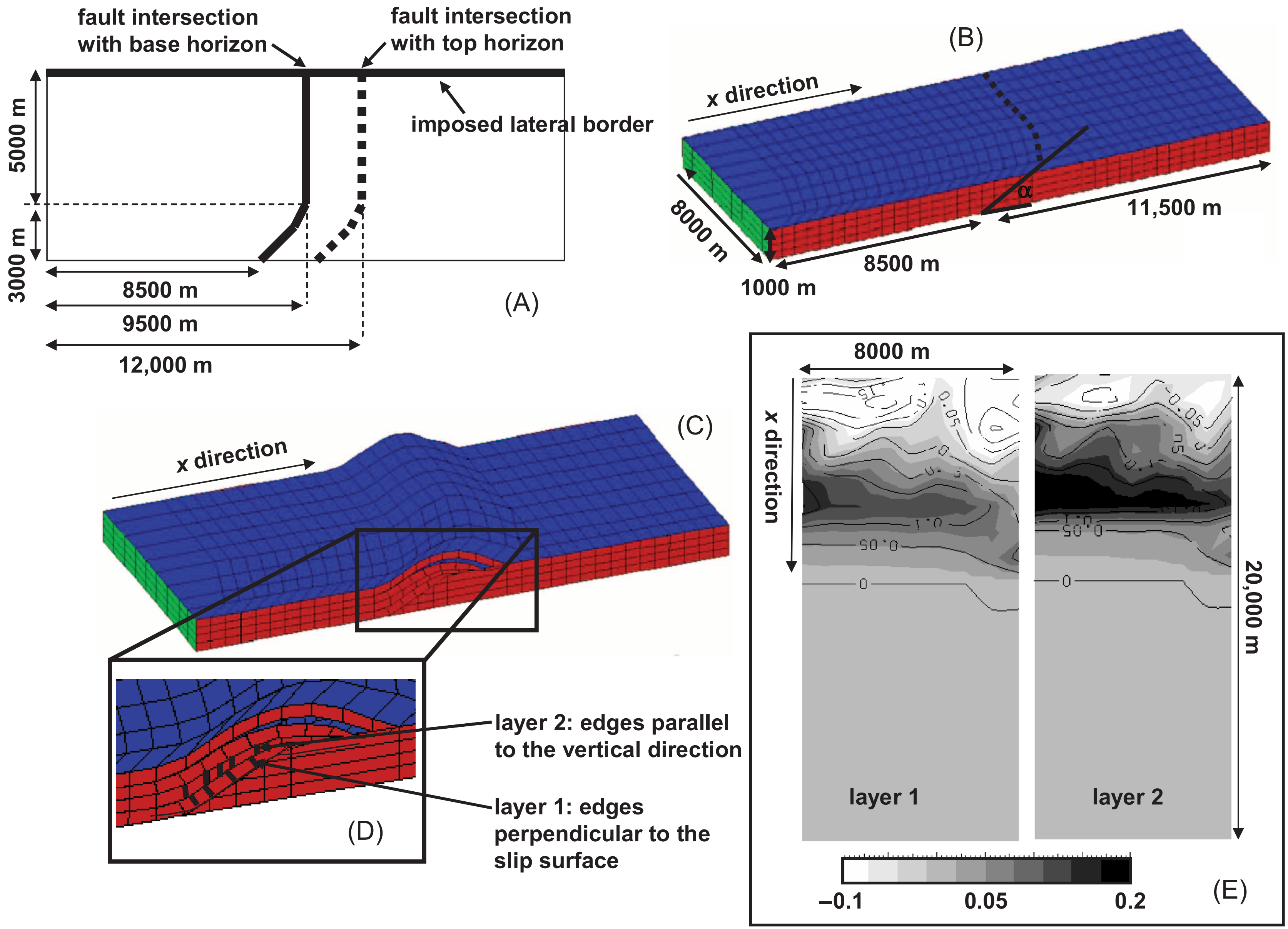

Figure 3. Combination of deformation mechanisms. (A) Top view of the initial 3-D model. (B) Perspective view of the initial 3-D model. (C) Perspective view of the deformed model after a displacement of 2000 m (6562 ft): the first and third layers are folded by flexural slip, the second and fourth layers are folded by vertical shear. (D) Enlargement of the deformed thrust unit. (E) Map view of the relative volumetric variation per cell for the first and the second layer.

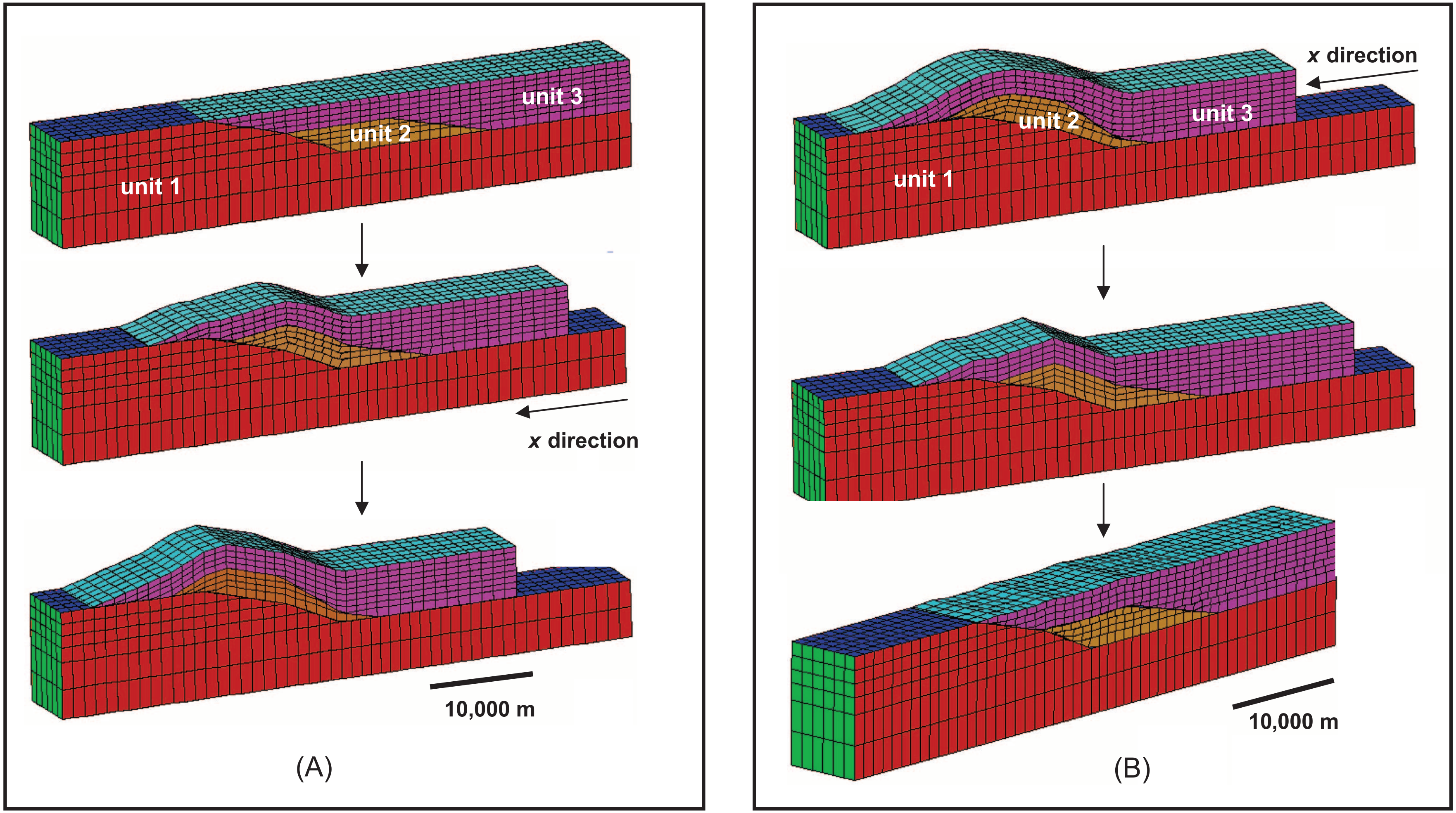

Figure 4. Reversibility validation. (A) Perspective view of the deformation of the model after two successive displacements of 3000 then 4000 m (9842 then 13,123 ft) in the *x* direction. (B) Perspective view of the model after two successive displacements of 5000 m (16,404 ft) to recover the deposition time.

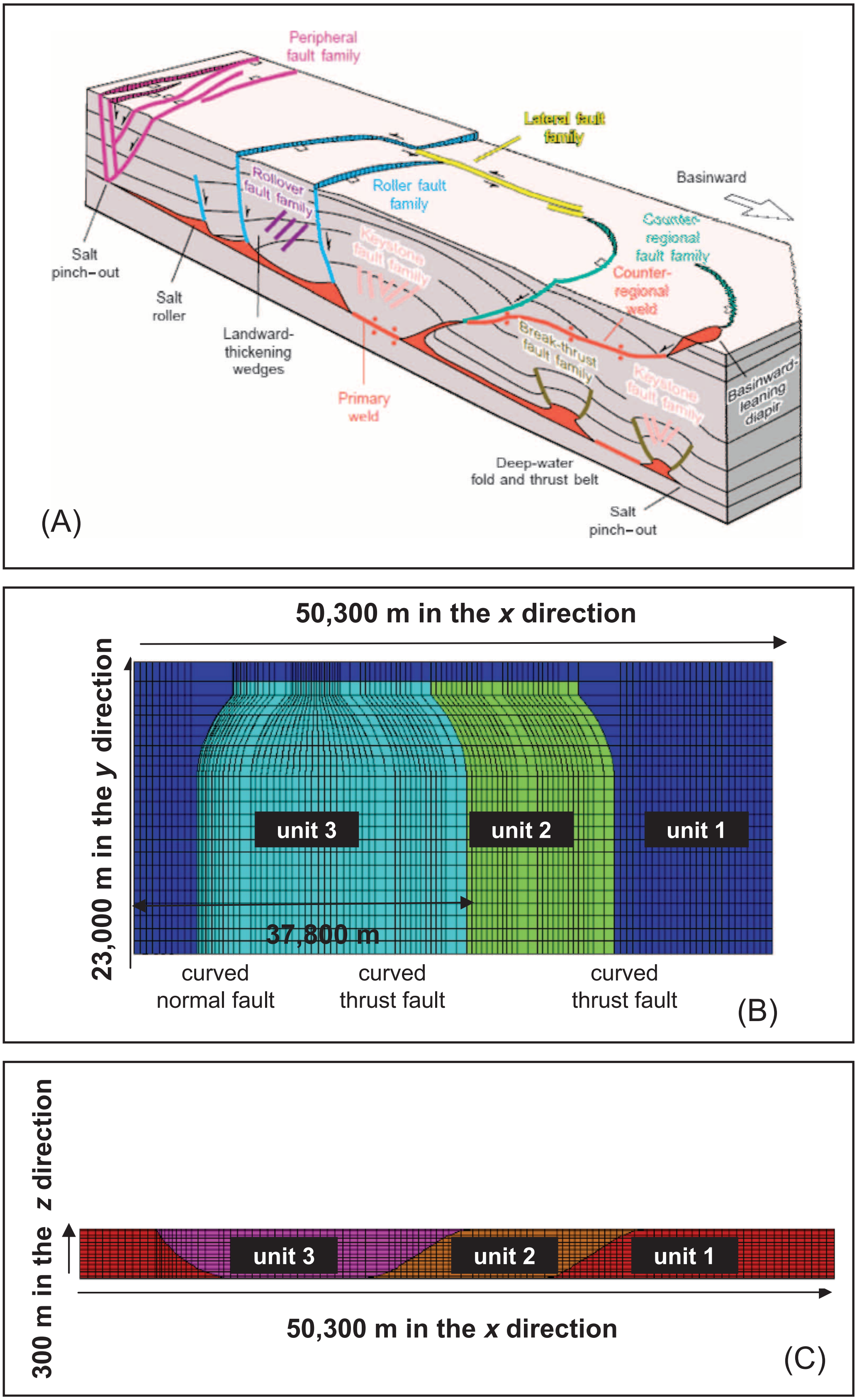

Figure 5. Complex structures with curved normal and thrust faults. (A) Schematic representation of the model with normal faults from Rowan et al. (1999) reprinted by permission of AAPG. (B) Bird's-eye view of the initial 3-D model. (C) Cross section representation of the initial 3-D model with units 2 and 3 and the basement (unit 1).

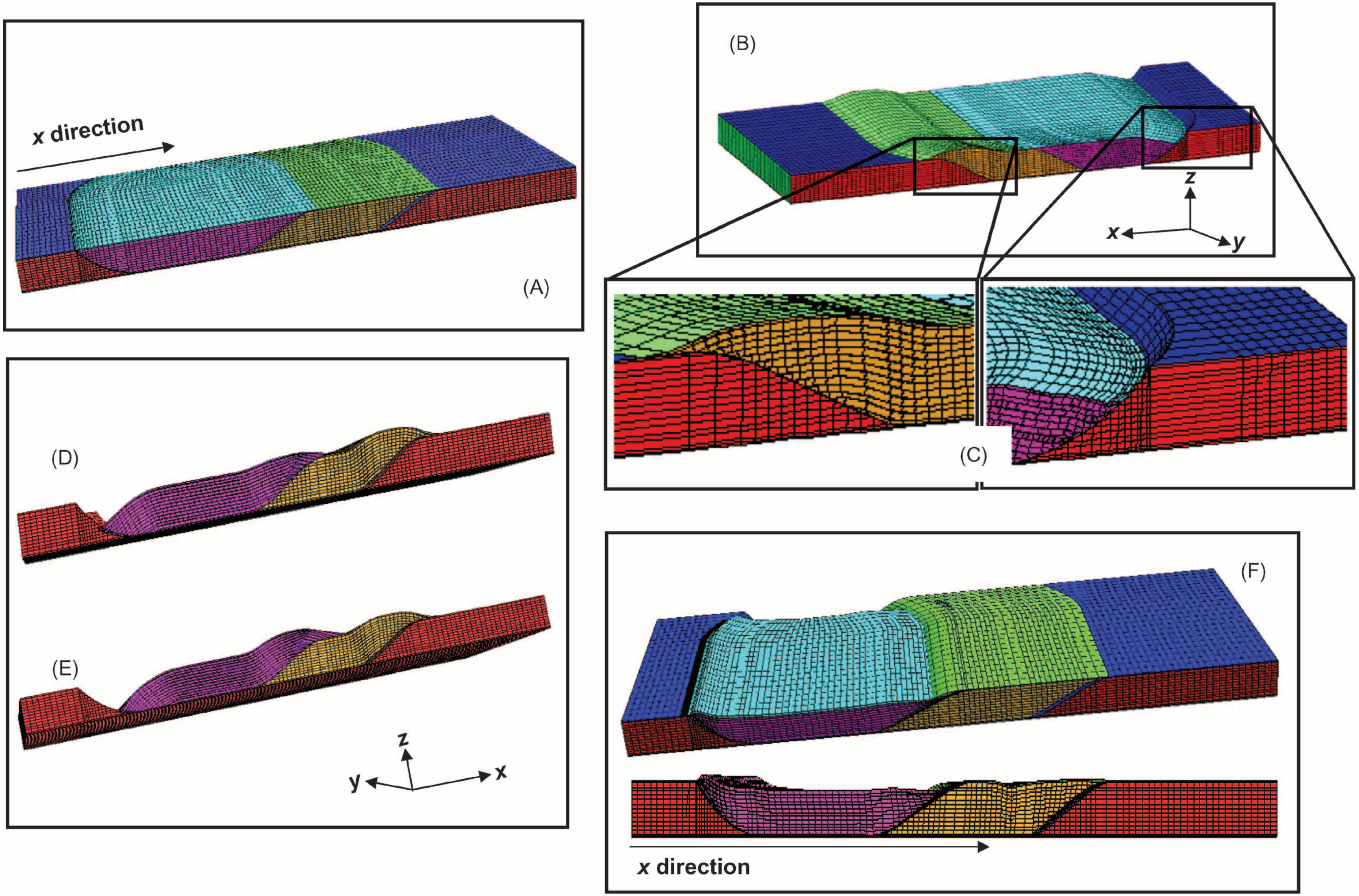

Figure 6. Deformation of the complex structure. (A) Perspective view of the initial gridded model. (B) Perspective view of the duplex (units 2 and 3) over the basement (unit 1) after a displacement of 2000 m (6562 ft). (C) Blow up of the deformation process near the normal and thrust faults. (D) Cross section view of successive displacements of the different units by flexural slip folding: the duplex (units 2 and 3) moves over the fixed basement (unit 1) by 2000 m (6562 ft), and then unit 3 moves over the fixed units (2 and 1) by 1000 m (3281 ft). (E) Cross section view of successive displacements of the different units by flexural slip folding: the duplex (units 2 and 3) moves over the basement (unit 1) by 2000 m (6562 ft) and then unit 3 moves over the fixed units (2 and 1) by 1800 m (5905 ft). (F) Perspective and cross section views of the restored state after a displacement of 2000 m (6562 ft) for units 2 and 3 and 1800 m (5905 ft) for unit 3.

2000 m (6562 ft). The fault surface between units 2 and 3 is not active at this step. Figure 6C shows an enlargement of the zone of deformation near the normal and thrust fault, attesting to the accuracy of the deformation. Figure 6D shows a more complex displacement sequence with successively a 2000-m (6562-ft) displacement of the duplex (units 2 + 3) over the fixed basement (unit 1) as in Figure 6B and then a 1000-m (3281-ft) displacement of unit 3 over the fixed units (1 + 2). Figure 6E shows the same sequence but with successively a 2000-m (6562-ft) displacement of the duplex (units 2 + 3) over fixed unit 1 and then a 1800-m (5905-ft) displacement of unit 3 over the fixed units (1 + 2). The approach used can consider a different value and direction for the displacement of each unit, which is not the case in this example. The results represent the folded structure with the inverse faults, and the perfect slip on the normal fault. This first example of realistic complexity demonstrates a step forward in 3-D basin modeling in a complex setting.

The reversibility of the approach was tested with this model (Figure 6E), and the results of the reverse problem are given in Figure 6F in perspective and cross-sectional views after a displacement of 2000 m (6562 ft) for units 2 + 3 and 1800 m (5905 ft) for unit 3. The results are consistent with the initial model before deformation. Reversibility is guaranteed because the mesh was defined initially with the constraints illustrated in equation 1. This demonstrates the necessity of building an appropriate meshed model suited to the restoration step. This example shows the originality of the approach and its potential for solving the problem in a reversible way on a single mesh.

DISCUSSION

Like every method aiming at modeling complex structural basins, our approach has certain advantages but also certain drawbacks and limitations. These are discussed below along with some possible improvements.

In the examples given, the lateral boundary conditions are vertical. However, the approach can integrate boundary limits of greater complexity such as a curved fault, for example. The integration of physical laws is more complex. Diagenetic compaction or erosion could be implemented by a kinematic algorithm with relatively simple geometrical rules, for example, by linking compaction with the depth of the cell, or erosion with the model surface slope. In contrast, the introduction of tectonic compaction (compaction linked to horizontal stress) needs to include some mechanics, which is a more difficult task. If the aim is to maintain a kinematic approach with large complex deformation and the advantage of hexahedral cells, one possibility is to identify certain steps in the progressive deformation where the stress distribution is calculated, by finite-element modeling for example, and to compute a modification in the shape of the elementary blocks by considering information on both stress and the mechanical properties of the rocks. This may be time consuming but it is reliable. Similarly, using fracture network simulators (Philip et al., 2005) at certain selected steps of the progressive deformation may help in evaluating changes in permeability.

A significant advantage of the model is its ability to consider multiscales from elementary rigid blocks (hexahedral cells of hectometric size) to duplexes of decakilometric size. However, this hypothesis requires sliding on the support surface to be perfect at the scale of the elementary blocks (size of the hexahedra). The concept of a thread fault, which is a smooth surface as close as possible to a thread, developed by Thibaut et al. (1997), could be used to check this assumption. A thread surface is a contact surface between two jointed blocks of rocks slipping on each other without deformation. Its description, based on a mechanical criterion, integrates the kinematic properties of slipping. Applying such a thread criterion to draw fault geometries more accurately at the scale of a rigid block drastically reduces the volumetric variation of the elementary cells. With such a criterion, the breaking point at the base of the ramp (Figure 2D) is smoothed and becomes curved. This reduces the volumetric variations in the cells as they climb the ramp to minimum values. Of course this criterion must not be applied at the scale of the entire fault:

ramps and curved faults exist in natural deformation and are responsible for deformation at kilometric and multikilometric scales (Figures 4, 6). This means that the roughness of a fault modeled with the thread criterion must be very low, only below the size of the elementary cells (decameter to hectometer size).

A second constraint for reversible kinematics is that the surfaces must be perfectly unfolded. When it is possible to identify flexural slip folding from geological observations (for example, from constant-length deformation markers), the geometry of such a layer must be such that it can be developed. In such cases, it is very useful to use an algorithm aimed at drawing the developable surface directly from the interpolator tool when building the model (Thibert et al., 2005). Not only are the developable layers better constrained, but the entire geological formation is also better balanced because flexural slip folding is more constraining, from a geometrical point of view, than simple shear folding.

A third constraint is that the building of the mesh should be reversible because it combines the advantage of a flexible mesh for solving the restoration problem with that of a structured grid for the deformation problem. It imposes constraints on the height and width of the cells as a function of the fault direction, the ramps, the curvature of the folds, and the displacement values. The mesh is complex to build and constrained. However, when it is created, it supports a precise and realistic basin description and is suitable for coupling with a basin fluid-flow simulator. The grid cells are structured for each layer such as they represent the stratigraphic time markers and lithostratigraphic characteristics. For a basin fluid-flow simulator that integrates the basin's thermal history, source rock expulsion history, and hydrocarbon fluid-flow migration (Ungerer et al., 1990), a hexahedral mesh is appropriate because the numerical solution for the flow-continuity and momentum equations integrating the fluid flux guarantees that the fluid mass is conserved at the interfaces between volumes of individual grid cells. Solving the problem with some tetrahedra would have been possible. This offers advantages in that flexible deformable grids can be employed, permitting the effective representation of discontinuities such as faults more easily. However, mass balance may be more difficult to maintain. In our approach, we offer an appropriate solution for both problems, restoration and coupling with a fluid-flow simulator.

CONCLUSIONS

Accessing new petroleum discoveries calls for continuous technological innovation. Fully integrated software solutions exist for predicting pressure, temperature history, and hydrocarbon generation in 2-D for complex structures (Schneider et al., 2002) and in 3-D for relatively simple geometries (Schneider, et al., 2000). In assessing petroleum systems, complex structures are defined as being faulted and folded, in which the paleogeometries cannot be described only by vertical deformation. The kinematic approach presented in this article demonstrates that possible solutions exist for solving the structural part of 3-D basin modeling in complex settings. This approach provides an incremental deformed geometry of the basin in space and in time. The meshed model based on hexahedra is fully appropriate for coupling with a basin fluid-flow simulator (Thibaut et al., 2007). The reversibility of the approach ensures the consistency of the discrete kinematic deformation path for the restoration and deformation steps. The approach offers different prospects for improvement. To integrate these different options, which have already been validated, one step forward would be to develop a software toolbox comprising all the different solutions to help future users build and constrain geological models more effectively. Consequently, future work should include the generalization of lateral boundary conditions and kinematic constraints such as a thread criterion to describe fault geometry better or some unfolding criterion for developable layers. It could also include mechanical constraints, inserted at some selected stage of progressive deformation such as compaction and erosion modeling and fracture network simulation to evaluate changes in physical parameters such as permeability and mass balance more accurately.

REFERENCES CITED

Bennis, C., J.-C. Lecomte, and M. Leger, 1995, Les algorithmes du calcul dans Patchwork: Institut Français du Pétrole Report, v. 41370, 21 p.

Caumont, G., F. Lepage, C. Sword, and J. L. Mallet, 2004, Building and editing a sealed geological model: Mathematical Geology, v. 36, p. 405–424, doi:10.1023/B:MATG.0000029297.18098.8a.

Cognot, R., J. L. Mallet, L. Souche, J. Massot, and L. Deny, 2001, Fiber based grid construction: Proceedings of the 21st Geological Object Computer Aided Design (GOCAD) Meeting, Nancy, France.

Contreras, J., and M. Suter, 1990, Kinematic modeling of cross sectional deformation sequences by computer simulation: Journal of Geophysics Research, v. 95, p. 21,913–21,929.

Cornu, T., F. Schneider, and J.-P. Gratier, 2003, 3-D discrete kinematic modeling applied to extensional and compressional tectonics, *in* D. Newland, ed., New insight into structural interpretation and modeling: Geological Society (London) Special Publication 212, p. 285–294.

Dewers, T., and P. Ortoleva, 1990, A coupled reaction/transport/mechanical model for intergranular pressure solution stylolites and differential compaction and cementation in clean sandstones: Geochimica et Cosmochimica Acta, v. 54, p. 1609–1625, doi:10.1016/0016-7037(90)90395-2.

Divies, R., 1997, Foldis: Un modèle cinématique de bassins sédimentaires par éléments discrets associant plis, failles, érosion/sédimentation et compaction: Ph.D. thesis, Université Joseph Fourier, Grenoble, France, 221 p.

Dunbar, J., and A. R. Cook, 2003, Palinspatic reconstruction of structure maps: An automate finite element approach with heterogeneous strains: Journal of Structural Geology, v. 25, p. 1021–1036, doi:10.1016/S0191-8141(02)00154-2.

Galera, C., C. Bennis, I. Moretti, and J.-J. Mallet, 2003, Construction of coherent 3-D geological blocs: Computers and Geosciences, v. 29, p. 971–984, doi:10.1016/S0098-3004(03)00085-2.

Gibbs, A., 1983, Balanced section constructions from seismic sections in areas of extensional tectonics: Journal of Structural Geology, v. 5, p. 153–160, doi:10.1016/0191-8141(83)90040-8.

Gibergues, N., 2007, Modélisation cinématique réversible 3D de structures géologiques plissées et faillées: Ph.D. thesis, Université Joseph Fourier, Grenoble, France, 86 p.

Gratier, J.-P., and F. Gueydan, 2007, Deformation in the presence of fluids and mineral reactions: Effect of fracturing and fluid-rocks interaction on seismic cycle, *in* M. R. Handy, G. Hirth, and N. Hovius, eds., Tectonic faults: Agent of change on a dynamic earth: Cambridge, Massachusetts, Dahlem Workshop, The MIT Press, p. 319–356.

Gratier, J.-P., and B. Guillier, 1993, Compatibility constraints on folded and faulted strata and calculation of the total displacement using computational restoration: Journal of Structural Geology, v. 15, p. 391–402, doi:10.1016/0191-8141(93)90135-W.

Gratier, J.-P., B. Guillier, A. Delorme, and F. Odonne, 1991, Restoration and balance of a folded and faulted surface by best-fitting of finite elements: Principle and applications: Journal of Structural Geology, v. 13, p. 111–115, doi:10.1016/0191-8141(91)90107-T.

Groshong, R. H., 1975, Strain, fractures, and pressure solution in natural single-layer folds: Geological Society of America Bulletin, v. 86, no. 10, p. 1363–1376, doi:10.1130/0016-7606(1975)86<1363:SFAPSI>2.0.CO;2.

Laubsher, H. B., 1975, Viscous components in Jura: Tectonophysics, v. 27, p. 239–254, doi:10.1016/0040-1951(75)90019-0.

Maerten, L., D. Pollard, and F. Maerten, 2001, Digital mapping of three-dimensional structures of Chimney Rock fault system, central Utah: Journal of Structural Geology, v. 23, p. 585–592, doi:10.1016/S0191-8141(00)00142-5.

Moretti, I., F. Lepage, and M. Guiton, 2006, Kine3D: A new 3-D restoration method based on a mixed approach linking geometry and geomechanics: Oil & Gas Science and Technology, v. 61, no. 2, p. 277–289.

Philip, Z. G., J. W. Jennings, J. E. Olson, S. E. Laubach, and J. Holder, 2005, Modeling coupled fracture-matrix fluid flow in geomechanically simulated fracture networks: Society of Petroleum Engineers Reservoir Evaluation and Engineering, v. 8, no. 4, p. 300–3009.

Ramsay, J. G., 1967, Folding and fracturing of rocks: New York, McGraw-Hill Book Company, 568 p.

Ramsay, J. G., and M. Huber, 1987, The technique of modern structural geology: Folds and fractures: London, Academic Press, v. 2, 700 p.

Rouby, D., P. R. Cobbold, P. Szatmari, S. Demercian, D. Coelho, and J. A. Rici, 1993, Least-squares palinspastic restoration of regions of normal faulting: Tectonophysics, v. 221, no. 3–4, p. 439–452, doi:10.1016/0040-1951(93)90172-G.

Rouby, D., H. Xiao, and J. Suppe, 2000, 3-D restoration of complexly folded and faulted surfaces using multiple unfolding mechanisms: AAPG Bulletin, v. 84, p. 805–829.

Rowan, M., M. P. Jackson, and B. Trudgill, 1999, Salt related fault families, and fault welds in the northern Gulf of Mexico: AAPG Bulletin, v. 83, p. 1454–1484.

Samson, P., 1996, Equilibrage de structures géologiques 3-D dans le cadre du projet GOCAD: Ph.D. thesis, Institut Polytechnique de Lorraine, Nancy, 223 p.

Schneider, F., S. Wolf, F. Faille, and D. Pot, 2000, A 3-D basin model for hydrocarbon potential basin evaluation: Application to Congo off shore: Oil & Gas Science and Technology, v. 55, no. 1, p. 3–13, doi:10.2516/ogst:2000001.

Schneider, F., H. Devoitine, I. Faille, E. Flauraud, and F. Willien, 2002, Ceres2D: A numerical prototype for HC potential evaluation in complex areas: Oil & Gas Science and Technology, v. 57, no. 6, p. 607–619, doi:10.2516/ogst:2002041.

Suppe, J., 1983, Geometry and kinematics of fault-bend folding: American Journal of Science, v. 283, p. 684–721.

Thibaut, M., J.-P. Gratier, M. Leger, and J.-M. Morvan, 1997, Least squares optimization of fault surfaces using the rigid block approximation: Journal of Structural Geology, v. 19, p. 735–743, doi:10.1016/S0191-8141(97)85678-7.

Thibaut, M., C. Sulzer, A. Jardin, and M. Bêche, 2007, ISBA: A methodological project for petroleum systems evaluation in complex areas: http://www.searchanddiscovery.com/documents/2007/08098thibaut/index.htm (accessed December 18, 2007).

Thibert, B., J.-P. Gratier, and J.-M. Morvan, 2005, A direct method for modeling developable strata and its geological application to Ventura Basin (California): Journal of Structural Geology, v. 27, p. 303–316, doi:10.1016/j.jsg.2004.08.011.

Ungerer, P., J. Burrus, B. Doligez, P. Y. Chénet, and F. Bessis, 1990, Basin evaluation by integrated two-dimensional modeling of heat transfer, fluid flow, hydrocarbon generation, and migration: AAPG Bulletin, v. 74, p. 309–335.

Williams, G. D., S. J. Kane, T. S. Buddin, and A. J. Richards, 1997, Restoration and balance of complex folded and faulted rock volumes: Flexural flattening, jigsaw fitting and decompaction in three dimensions: Tectonophysics, v. 273, no. 3–4, p. 203–218 , doi:10.1016/S0040-1951(96)00282-X.